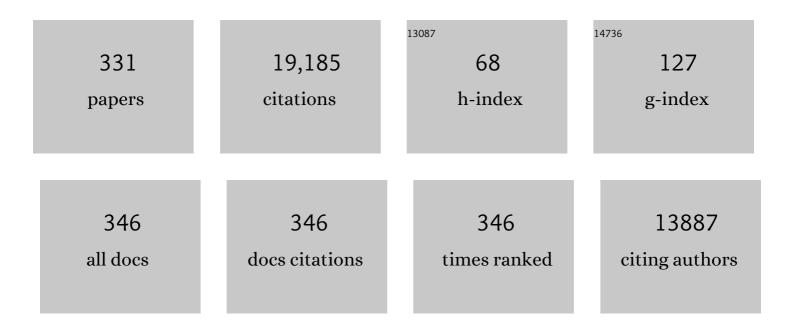
List of Publications by Year in descending order

Source: https://exaly.com/author-pdf/3810769/publications.pdf Version: 2024-02-01



#	Article	IF	CITATIONS
1	Microstructural evolution during film growth. Journal of Vacuum Science and Technology A: Vacuum, Surfaces and Films, 2003, 21, S117-S128.	0.9	1,466
2	Stretchable batteries with self-similar serpentine interconnects and integrated wireless recharging systems. Nature Communications, 2013, 4, 1543.	5.8	1,169
3	A novel pulsed magnetron sputter technique utilizing very high target power densities. Surface and Coatings Technology, 1999, 122, 290-293.	2.2	910
4	Development of preferred orientation in polycrystalline TiN layers grown by ultrahigh vacuum reactive magnetron sputtering. Applied Physics Letters, 1995, 67, 2928-2930.	1.5	366
5	Pathways of atomistic processes on TiN(001) and (111) surfaces during film growth: anab initiostudy. Journal of Applied Physics, 2003, 93, 9086-9094.	1.1	318
6	Microstructure modification of TiN by ion bombardment during reactive sputter deposition. Thin Solid Films, 1989, 169, 299-314.	0.8	308
7	Growth of Semiconducting Graphene on Palladium. Nano Letters, 2009, 9, 3985-3990.	4.5	307
8	Surface changes on LiNi0.8Co0.2O2 particles during testing of high-power lithium-ion cells. Electrochemistry Communications, 2002, 4, 620-625.	2.3	295
9	Detection of Single Atoms and Buried Defects in Three Dimensions by Aberration-Corrected Electron Microscope with 0.5-A Information Limit. Microscopy and Microanalysis, 2008, 14, 469-477.	0.2	266
10	Interface microstructure engineering by high power impulse magnetron sputtering for the enhancement of adhesion. Journal of Applied Physics, 2007, 101, 054301.	1.1	247
11	High power pulsed magnetron sputtered CrN films. Surface and Coatings Technology, 2003, 163-164, 267-272.	2.2	242
12	Ionized sputter deposition using an extremely high plasma density pulsed magnetron discharge. Journal of Vacuum Science and Technology A: Vacuum, Surfaces and Films, 2000, 18, 1533-1537.	0.9	235
13	Highâ€flux lowâ€energy (â‰,20 eV) N+2ion irradiation during TiN deposition by reactive magnetron sputtering: Effects on microstructure and preferred orientation. Journal of Applied Physics, 1995, 78, 5395-5403.	1.1	229
14	Microscopy and Spectroscopy of Lithium Nickel Oxide-Based Particles Used in High Power Lithium-Ion Cells. Journal of the Electrochemical Society, 2003, 150, A1450.	1.3	219
15	Growth of poly- and single-crystal ScN on MgO(001): Role of low-energy N2+ irradiation in determining texture, microstructure evolution, and mechanical properties. Journal of Applied Physics, 1998, 84, 6034-6041.	1.1	218
16	Polycrystalline TiN films deposited by reactive bias magnetron sputtering: Effects of ion bombardment on resputtering rates, film composition, and microstructure. Journal of Vacuum Science and Technology A: Vacuum, Surfaces and Films, 1992, 10, 265-272.	0.9	208
17	Average energy deposited per atom: A universal parameter for describing ionâ€essisted film growth?. Applied Physics Letters, 1993, 63, 36-38.	1.5	206
18	Crystal growth and microstructure of polycrystalline Ti1â^'xAlxN alloy films deposited by ultra-high-vacuum dual-target magnetron sputtering. Thin Solid Films, 1993, 235, 62-70.	0.8	193

#	Article	IF	CITATIONS
19	Self-organized nanocolumnar structure in superhard TiB2 thin films. Applied Physics Letters, 2005, 86, 131909.	1.5	192
20	Highly Sensitive, Mechanically Stable Nanopore Sensors for DNA Analysis. Advanced Materials, 2009, 21, 2771-2776.	11.1	190
21	Microstructure and oxidation-resistance of Ti1 â^' x â^' y â^'zAlxCryYzN layers grown by combined steered-arc/unbalanced-magnetron-sputter deposition. Surface and Coatings Technology, 1997, 94-95, 226-231.	2.2	189
22	Synthesis of metastable epitaxial zincâ€blendeâ€structure AlN by solidâ€state reaction. Applied Physics Letters, 1992, 60, 2491-2493.	1.5	187
23	Use of an externally applied axial magnetic field to control ion/neutral flux ratios incident at the substrate during magnetron sputter deposition. Journal of Vacuum Science and Technology A: Vacuum, Surfaces and Films, 1992, 10, 3283-3287.	0.9	179
24	Mass and energy resolved detection of ions and neutral sputtered species incident at the substrate during reactive magnetron sputtering of Ti in mixed Ar+N2 mixtures. Journal of Vacuum Science and Technology A: Vacuum, Surfaces and Films, 1994, 12, 2846-2854.	0.9	178
25	Long-Range and Local Structure in the Layered Oxide Li _{1.2} Co _{0.4} Mn _{0.4} O ₂ . Chemistry of Materials, 2011, 23, 2039-2050.	3.2	171
26	Effects of highâ€flux lowâ€energy (20–100 eV) ion irradiation during deposition on the microstructure and preferred orientation of Ti0.5Al0.5N alloys grown by ultraâ€highâ€vacuum reactive magnetron sputtering. Journal of Applied Physics, 1993, 73, 8580-8589.	1.1	159
27	Interpretation of X-ray photoelectron spectra of carbon-nitride thin films: New insights from in situ XPS. Carbon, 2016, 108, 242-252.	5.4	158
28	Lowâ€energy (â^1⁄4100 eV) ion irradiation during growth of TiN deposited by reactive magnetron sputtering: Effects of ion flux on film microstructure. Journal of Vacuum Science and Technology A: Vacuum, Surfaces and Films, 1991, 9, 434-438.	0.9	157
29	Local Structure of Layered Oxide Electrode Materials for Lithiumâ€lon Batteries. Advanced Materials, 2010, 22, 1122-1127.	11.1	152
30	Vacancy hardening in single-crystal TiNx(001) layers. Journal of Applied Physics, 2003, 93, 6025-6028.	1.1	146
31	Interface structure in superhard TiN-SiN nanolaminates and nanocomposites: Film growth experiments andab initiocalculations. Physical Review B, 2007, 75, .	1.1	142
32	Defect structure and phase transitions in epitaxial metastable cubic Ti0.5Al0.5N alloys grown on MgO(001) by ultraâ€highâ€vacuum magnetron sputter deposition. Journal of Applied Physics, 1991, 69, 6437-6450.	1.1	141
33	Local structure and composition studies of Li1.2Ni0.2Mn0.6O2 by analytical electron microscopy. Journal of Power Sources, 2008, 178, 422-433.	4.0	141
34	Electronic structure of ScN determined using optical spectroscopy, photoemission, andab initiocalculations. Physical Review B, 2001, 63, .	1.1	139
35	Improving high-capacity Li1.2Ni0.15Mn0.55Co0.1O2-based lithium-ion cells by modifiying the positive electrode with alumina. Journal of Power Sources, 2013, 233, 346-357.	4.0	139
36	Structure determination of individual single-wall carbon nanotubes by nanoarea electron diffraction. Applied Physics Letters, 2003, 82, 2703-2705.	1.5	137

#	Article	IF	CITATIONS
37	Electrochemically tunable thermal conductivity of lithium cobalt oxide. Nature Communications, 2014, 5, 4035.	5.8	137
38	Dense fully 111-textured TiN diffusion barriers: Enhanced lifetime through microstructure control during layer growth. Journal of Applied Physics, 1999, 86, 3633-3641.	1.1	125
39	Physico-chemical characterization of NF/RO membrane active layers by Rutherford backscattering spectrometrya `†. Journal of Membrane Science, 2006, 282, 71-81.	4.1	120
40	Role of Tin+ and Aln+ ion irradiation (n=1, 2) during Ti1-xAlxN alloy film growth in a hybrid HIPIMS/magnetron mode. Surface and Coatings Technology, 2012, 206, 4202-4211.	2.2	119
41	Growth, surface morphology, and electrical resistivity of fully strained substoichiometric epitaxial TiNx (0.67⩽x<1.0) layers on MgO(001). Journal of Applied Physics, 2004, 95, 356-362.	1.1	118
42	Ion-assisted growth of Ti1â^'xAlxN/Ti1â^'yNbyN multilayers by combined cathodic-arc/magnetron-sputter deposition. Thin Solid Films, 1997, 302, 179-192.	0.8	117
43	Growth of single-crystal CrN on MgO(001): Effects of low-energy ion-irradiation on surface morphological evolution and physical properties. Journal of Applied Physics, 2002, 91, 3589-3597.	1.1	117
44	Band gap in epitaxial NaCl-structure CrN(001) layers. Journal of Applied Physics, 2002, 91, 5882-5886.	1.1	117
45	Microstructure and electronic properties of the refractory semiconductor ScN grown on MgO(001) by ultra-high-vacuum reactive magnetron sputter deposition. Journal of Vacuum Science and Technology A: Vacuum, Surfaces and Films, 1998, 16, 2411-2417.	0.9	112
46	Diagnosis of power fade mechanisms in high-power lithium-ion cells. Journal of Power Sources, 2003, 119-121, 511-516.	4.0	110
47	Phase composition and microstructure of polycrystalline and epitaxial TaNx layers grown on oxidized Si(001) and MgO(001) by reactive magnetron sputter deposition. Thin Solid Films, 2002, 402, 172-182.	0.8	109
48	Toughness enhancement in hard ceramic thin films by alloy design. APL Materials, 2013, 1, .	2.2	109
49	Metal versus rare-gas ion irradiation during Ti1â^' <i>x</i> Al <i>x</i> N film growth by hybrid high power pulsed magnetron/dc magnetron co-sputtering using synchronized pulsed substrate bias. Journal of Vacuum Science and Technology A: Vacuum, Surfaces and Films, 2012, 30, .	0.9	98
50	Epitaxial and polycrystalline HfNx (0.8⩽x⩽1.5) layers on MgO(001): Film growth and physical properties. Journal of Applied Physics, 2005, 97, 083521.	1.1	95
51	Paradigm shift in thin-film growth by magnetron sputtering: From gas-ion to metal-ion irradiation of the growing film. Journal of Vacuum Science and Technology A: Vacuum, Surfaces and Films, 2019, 37, .	0.9	94
52	Nanomachining carbon nanotubes with ion beams. Applied Physics Letters, 2004, 84, 4484-4486.	1.5	92
53	Epitaxial NaCl structure δ-TaNx(001): Electronic transport properties, elastic modulus, and hardness versus N/Ta ratio. Journal of Applied Physics, 2001, 90, 2879-2885.	1.1	88
54	Development of preferred orientation in polycrystalline NaCl-structure δ-TaN layers grown by reactive magnetron sputtering: Role of low-energy ion surface interactions. Journal of Applied Physics, 2002, 92, 5084-5093.	1.1	87

#	Article	IF	CITATIONS
55	Epitaxial Sc1â^'xTixN(001): Optical and electronic transport properties. Journal of Applied Physics, 2001, 89, 401-409.	1.1	84
56	Growth and physical properties of epitaxial HfN layers on MgO(001). Journal of Applied Physics, 2004, 96, 878-884.	1.1	83
57	Transmission electron microscopy studies of microstructural evolution, defect structure, and phase transitions in polycrystalline and epitaxial Ti1â°'xAlxN and TiN films grown by reactive magnetron sputter deposition. Thin Solid Films, 1991, 205, 153-164.	0.8	80
58	Coherent nano-area electron diffraction. Microscopy Research and Technique, 2004, 64, 347-355.	1.2	79
59	Morphology of epitaxial TiN(001) grown by magnetron sputtering. Applied Physics Letters, 1997, 70, 1703-1705.	1.5	78
60	Elastic constants of single-crystalTiNx(001)(0.67⩽x⩽1.0)determined as a function ofxby picosecond ultrasonic measurements. Physical Review B, 2005, 71, .	1.1	78
61	Moiré Superstructures of Graphene on Faceted Nickel Islands. ACS Nano, 2010, 4, 6509-6514.	7.3	78
62	Vacancy-induced toughening in hard single-crystal V 0.5 Mo 0.5 N x /MgO(0 0 1) thin films. Acta Materialia, 2014, 77, 394-400.	3.8	75
63	Multiscale Modeling of Thin-Film Deposition: Applications to Si Device Processing. MRS Bulletin, 2001, 26, 182-189.	1.7	74
64	Hydrogen uptake in alumina thin films synthesized from an aluminum plasma stream in an oxygen ambient. Applied Physics Letters, 1999, 74, 200-202.	1.5	73
65	Transfer of graphene layers grown on SiC wafers to other substrates and their integration into field effect transistors. Applied Physics Letters, 2009, 95, .	1.5	71
66	Dynamic and structural stability of cubic vanadium nitride. Physical Review B, 2015, 91, .	1.1	71
67	A review of the intrinsic ductility and toughness of hard transition-metal nitride alloy thin films. Thin Solid Films, 2019, 688, 137479.	0.8	71
68	Probing Interfacial Electronic Structures in Atomic Layer LaMnO ₃ and SrTiO ₃ Superlattices. Advanced Materials, 2010, 22, 1156-1160.	11.1	69
69	Strain-free, single-phase metastable Ti0.38Al0.62N alloys with high hardness: metal-ion energy vs. momentum effects during film growth by hybrid high-power pulsed/dc magnetron cosputtering. Thin Solid Films, 2014, 556, 87-98.	0.8	69
70	Microstructural evolution and Poisson ratio of epitaxial ScN grown on TiN(001)/MgO(001) by ultrahigh vacuum reactive magnetron sputter deposition. Journal of Applied Physics, 1999, 86, 5524-5529.	1.1	68
71	Structural study of Li2MnO3 by electron microscopy. Journal of Materials Science, 2009, 44, 5579-5587.	1.7	68
72	Large-scale fabrication of hard superlattice thin films by combined steered arc evaporation and unbalanced magnetron sputtering. Surface and Coatings Technology, 1997, 93, 69-87.	2.2	67

#	Article	IF	CITATIONS
73	Influence of the bias voltage on the structure and the tribological performance of nanoscale multilayer C/Cr PVD coatings. Thin Solid Films, 2005, 475, 219-226.	0.8	66
74	Selection of metal ion irradiation for controlling Ti1â^'xAlxN alloy growth via hybrid HIPIMS/magnetron co-sputtering. Vacuum, 2012, 86, 1036-1040.	1.6	66
75	Growth and physical properties of epitaxial metastable cubic TaN(001). Applied Physics Letters, 1999, 75, 3808-3810.	1.5	65
76	Layer-by-Layer Transfer of Multiple, Large Area Sheets of Graphene Grown in Multilayer Stacks on a Single SiC Wafer. ACS Nano, 2010, 4, 5591-5598.	7.3	65
77	Analytical electron microscopy of Li1.2Co0.4Mn0.4O2 for lithium-ion batteries. Solid State Ionics, 2011, 182, 98-107.	1.3	65
78	Improving the high-temperature oxidation resistance of TiB2 thin films by alloying with Al. Acta Materialia, 2020, 196, 677-689.	3.8	65
79	Electrostatic Probe Measurements in the Glow Discharge Plasma of a D. C. Magnetron Sputtering System. Contributions To Plasma Physics, 1988, 28, 157-167.	0.5	62
80	In situ Transmission Electron Microscopy Studies Enabled by Microelectromechanical System Technology. Journal of Materials Research, 2005, 20, 1802-1807.	1.2	60
81	Influence of an external axial magnetic field on the plasma characteristics and deposition conditions during direct current planar magnetron sputtering. Journal of Vacuum Science and Technology A: Vacuum, Surfaces and Films, 1994, 12, 314-320.	0.9	58
82	Highly oriented ZnO films obtained by d.c. reactive sputtering of a zinc target. Thin Solid Films, 1984, 120, 55-67.	0.8	57
83	Synthesis of linked carbon monolayers: Films, balloons, tubes, and pleated sheets. Proceedings of the National Academy of Sciences of the United States of America, 2008, 105, 7353-7358.	3.3	57
84	Physical properties of epitaxial ZrN/MgO(001) layers grown by reactive magnetron sputtering. Journal of Vacuum Science and Technology A: Vacuum, Surfaces and Films, 2013, 31, .	0.9	56
85	Effects of phase stability, lattice ordering, and electron density on plastic deformation in cubic TiWN pseudobinary transition-metal nitride alloys. Acta Materialia, 2016, 103, 823-835.	3.8	56
86	Dependence of the electromechanical coupling on the degree of orientation of c-textured thin AlN films. IEEE Transactions on Ultrasonics, Ferroelectrics, and Frequency Control, 2004, 51, 1347-1353.	1.7	55
87	Comparison of magnetron sputter deposition conditions in neon, argon, krypton, and xenon discharges. Journal of Vacuum Science and Technology A: Vacuum, Surfaces and Films, 1993, 11, 2733-2741.	0.9	54
88	Epitaxial Ti1-xWxN alloys grown on MgO(001) by ultrahigh vacuum reactive magnetron sputtering: Electronic properties and long-range cation ordering. Journal of Vacuum Science and Technology A: Vacuum, Surfaces and Films, 2003, 21, 140-146.	0.9	54
89	Raman scattering from TiNx (0.67 â‰≇€‰x â‰≇€‰1.00) single crystals grown on MgO(001). Journa Physics, 2011, 110, .	al of Applied	d ₅₄
90	Control of Ti1â^'xSixN nanostructure via tunable metal-ion momentum transfer during HIPIMS/DCMS co-deposition. Surface and Coatings Technology, 2015, 280, 174-184.	2.2	53

#	Article	IF	CITATIONS
91	Interfacial reactions in single-crystal-TiN (100)/Al/polycrystalline-TiN multilayer thin films. Thin Solid Films, 1992, 215, 152-161.	0.8	52
92	Improved Ti ₁ –xAl _x N PVD Coatings for Dry High Speed Cutting Operations. Surface Engineering, 1998, 14, 37-42.	1.1	52
93	Epitaxial Ti2AlN(0001) thin film deposition by dual-target reactive magnetron sputtering. Acta Materialia, 2007, 55, 4401-4407.	3.8	52
94	Ab initio and classical molecular dynamics simulations of N2 desorption from TiN(001) surfaces. Surface Science, 2014, 624, 25-31.	0.8	52
95	Determining absolute orientation-dependent step energies: a general theory for the Wulff-construction and for anisotropic two-dimensional island shape fluctuations. Surface Science, 2003, 522, 75-83.	0.8	50
96	Thermally induced self-hardening of nanocrystalline Ti–B–N thin films. Journal of Applied Physics, 2006, 100, 044301.	1.1	50
97	Conjugated Carbon Monolayer Membranes: Methods for Synthesis and Integration. Advanced Materials, 2010, 22, 1072-1077.	11.1	50
98	Thermal stability of carbon nitride thin films. Journal of Materials Research, 2001, 16, 3188-3201.	1.2	49
99	Elastic constants, Poisson ratios, and the elastic anisotropy of VN(001), (011), and (111) epitaxial layers grown by reactive magnetron sputter deposition. Journal of Applied Physics, 2014, 115, 214908.	1.1	49
100	TiN(001) and TiN(111) island coarsening kinetics: in-situ scanning tunneling microscopy studies. Thin Solid Films, 2001, 392, 164-168.	0.8	48
101	Dynamics of Ti, N, and TiN <mmi:math <br="" xmins:mmi="http://www.w3.org/1998/Math/MathML">display="inline"><mml:msub><mml:mrow></mml:mrow><mml:mi>x</mml:mi></mml:msub>(<mml:math) et<="" td="" tj=""><td>Qq1 1 0.7 1.1</td><td>′84314 rgBT 47</td></mml:math)></mmi:math>	Qq1 1 0.7 1.1	′84314 rgBT 47
102	admolecule transport on TiW(001) surfaces. Physical Review B, 2012, 86, . Controlling the B/Ti ratio of TiBx thin films grown by high-power impulse magnetron sputtering. Journal of Vacuum Science and Technology A: Vacuum, Surfaces and Films, 2018, 36, .	0.9	46
103	Adaptive hard and tough mechanical response in single-crystal B1 VNx ceramics via control of anion vacancies. Acta Materialia, 2020, 192, 78-88.	3.8	46
104	Effects of an unbalanced magnetron in a unique dual-cathode, high rate reactive sputtering system. Thin Solid Films, 1990, 193-194, 117-126.	0.8	45
105	Enhanced adhesion through local epitaxy of transition-metal nitride coatings on ferritic steel promoted by metal ion etching in a combined cathodic arc/unbalanced magnetron deposition system. Journal of Vacuum Science and Technology A: Vacuum, Surfaces and Films, 2000, 18, 1718-1723.	0.9	45
106	Nucleation kinetics during homoepitaxial growth of TiN(001) by reactive magnetron sputtering. Physical Review B, 2004, 70, .	1.1	45
107	Novel strategy for low-temperature, high-rate growth of dense, hard, and stress-free refractory ceramic thin films. Journal of Vacuum Science and Technology A: Vacuum, Surfaces and Films, 2014, 32,	0.9	45
108	Effect of WN content on toughness enhancement in V1â^'xWxN/MgO(001) thin films. Journal of Vacuum Science and Technology A: Vacuum, Surfaces and Films, 2014, 32, .	0.9	45

#	Article	IF	CITATIONS
109	Elastic properties and plastic deformation of TiC- and VC-based pseudobinary alloys. Acta Materialia, 2018, 144, 376-385.	3.8	45
110	Absolute orientation-dependent TiN() step energies from two-dimensional equilibrium island shape and coarsening measurements on epitaxial TiN() layers. Surface Science, 2002, 513, 468-474.	0.8	44
111	Phase separation and formation of the self-organised layered nanostructure in C/Cr coatings in conditions of high ion irradiation. Surface and Coatings Technology, 2005, 200, 1572-1579.	2.2	42
112	Two-dimensional island dynamics: Role of step energy anisotropy. Surface Science Reports, 2006, 60, 55-77.	3.8	42
113	Electronic structure of the SiN <mml:math <br="" xmlns:mml="http://www.w3.org/1998/Math/MathML">display="inline"><mml:mrow><mml:msub><mml:mrow /><mml:mrow><mml:mi>x</mml:mi></mml:mrow></mml:mrow </mml:msub></mml:mrow></mml:math> /TiN interface: A model system for superhard nanocomposites. Physical Review B. 2011. 83	1.1	42
114	Strategy for simultaneously increasing both hardness and toughness in ZrB2-rich Zr1â^'xTaxBy thin films. Journal of Vacuum Science and Technology A: Vacuum, Surfaces and Films, 2019, 37, .	0.9	42
115	Interfacial reactions in epitaxial Al/Ti1â^'xAlxN (0≤â‰0.2) model diffusionâ€barrier structures. Journal of Vacuum Science and Technology A: Vacuum, Surfaces and Films, 1993, 11, 11-17.	0.9	41
116	Nitrogen-doped bcc-Cr films: Combining ceramic hardness with metallic toughness and conductivity. Scripta Materialia, 2016, 122, 40-44.	2.6	41
117	Epitaxial growth of metastable Î-TaN layers on MgO(001) using low-energy, high-flux ion irradiation during ultrahigh vacuum reactive magnetron sputtering. Journal of Vacuum Science and Technology A: Vacuum, Surfaces and Films, 2002, 20, 2007.	0.9	40
118	Absolute orientation-dependent anisotropic TiN(111) island step energies and stiffnesses from shape fluctuation analyses. Physical Review B, 2003, 67, .	1.1	40
119	Ti adatom diffusion on TiN(001): Ab initio and classical molecular dynamics simulations. Surface Science, 2014, 627, 34-41.	0.8	40
120	Controlling the boron-to-titanium ratio in magnetron-sputter-deposited TiBx thin films. Journal of Vacuum Science and Technology A: Vacuum, Surfaces and Films, 2017, 35, .	0.9	40
121	Effects of high-flux low-energy ion bombardment on the low-temperature growth morphology of TiN(001) epitaxial layers. Physical Review B, 2000, 61, 16137-16143.	1.1	39
122	Ab Initio Molecular Dynamics Simulations of Nitrogen/VN(001) Surface Reactions: Vacancy-Catalyzed N ₂ Dissociative Chemisorption, N Adatom Migration, and N ₂ Desorption. Journal of Physical Chemistry C, 2016, 120, 12503-12516.	1.5	39
123	3D-to-2D Morphology Manipulation of Sputter-Deposited Nanoscale Silver Films on Weakly Interacting Substrates via Selective Nitrogen Deployment for Multifunctional Metal Contacts. ACS Applied Nano Materials, 2020, 3, 4728-4738.	2.4	38
124	In situ high-temperature scanning tunneling microscopy studies of two-dimensional TiN island coarsening kinetics on TiN. Surface Science, 2003, 526, 85-96.	0.8	37
125	Dislocation-driven surface dynamics on solids. Nature, 2004, 429, 49-52.	13.7	37
126	Nucleation kinetics versus nitrogen partial pressure during homoepitaxial growth of stoichiometric TiN(001): A scanning tunneling microscopy study. Surface Science, 2005, 581, L122-127.	0.8	37

#	Article	IF	CITATIONS
127	Synergistic Compositions of Colloidal Nanodiamond as Lubricant-additive. Journal of Vacuum Science and Technology B:Nanotechnology and Microelectronics, 2010, 28, 869-877.	0.6	37
128	Design and characterization of a compact twoâ€ŧarget ultrahigh vacuum magnetron sputter deposition system: Application to the growth of epitaxial Ti1â^'xAlxN alloys and TiN/Ti1â^'xAlxN superlattices. Journal of Vacuum Science and Technology A: Vacuum, Surfaces and Films, 1993, 11, 136-142.	0.9	36
129	Absolute TiN(111) Step Energies from Analysis of Anisotropic Island Shape Fluctuations. Physical Review Letters, 2002, 88, 146101.	2.9	36
130	Measurement and estimation of temperature rise in TEM sample during ion milling. Ultramicroscopy, 2007, 107, 663-668.	0.8	36
131	Raman scattering from epitaxial TaNx(0.94≤â‰≇.37) layers grown on MgO(001). Journal of Applied Physics, 2007, 101, 123509.	1.1	35
132	Nanolabyrinthine ZrAlN thin films by self-organization of interwoven single-crystal cubic and hexagonal phases. APL Materials, 2013, 1, .	2.2	35
133	Strategy for tuning the average charge state of metal ions incident at the growing film during HIPIMS deposition. Vacuum, 2015, 116, 36-41.	1.6	34
134	Phonon and electron contributions to the thermal conductivity of <mml:math xmlns:mml="http://www.w3.org/1998/Math/MathML"><mml:mrow><mml:mi mathvariant="normal">V<mml:msub><mml:mi mathvariant="normal">N<mml:mi>x</mml:mi></mml:mi </mml:msub></mml:mi </mml:mrow> epitaxial layers. Physical Review Materials, 2017, 1, .</mml:math 	0.9	34
135	Origin of compositional variations in sputterâ€deposited TixW1â^'x diffusion barrier layers. Applied Physics Letters, 1995, 67, 3102-3104.	1.5	33
136	Structure and tribological behaviour of nanoscale multilayer C/Cr coatings deposited by the combined steered cathodic arc/unbalanced magnetron sputtering technique. Thin Solid Films, 2004, 447,448, 7-13.	0.8	33
137	xmlns:mml="http://www.w3.org/1998/Math/MathML" display="inline"> <mml:msub><mml:mrow /><mml:mrow><mml:mn>1</mml:mn><mml:mo>â^`</mml:mo><mml:mi>x</mml:mi></mml:mrow>xmlns:mml="http://www.w3.org/1998/Math/MathML" display="inline"><mml:mi>x</mml:mi></mml:mrow </mml:msub> <mml:mrow /><mml:mi>x</mml:mi>N(001) surfaces from first principles. Physical Review</mml:mrow 	> 1.1	athၟၖၟAl <mnil:< td=""></mnil:<>
138	B, 2012, 85, . Al capping layers for nondestructive x-ray photoelectron spectroscopy analyses of transition-metal nitride thin films. Journal of Vacuum Science and Technology A: Vacuum, Surfaces and Films, 2015, 33, .	0.9	33
139	Microstructure and materials properties of understoichiometric TiBx thin films grown by HiPIMS. Surface and Coatings Technology, 2020, 404, 126537.	2.2	33
140	Size-Dependent Detachment-Limited Decay Kinetics of Two-Dimensional TiN Islands on TiN(111). Physical Review Letters, 2002, 89, 176102.	2.9	32
141	Low-energy electron microscopy studies of interlayer mass transport kinetics on TiN(111). Surface Science, 2004, 560, 53-62.	0.8	32
142	The Formation and Utility of Sub-Angstrom to Nanometer-Sized Electron Probes in the Aberration-Corrected Transmission Electron Microscope at the University of Illinois. Microscopy and Microanalysis, 2010, 16, 183-193.	0.2	32
143	N and Ti adatom dynamics on stoichiometric polar TiN(111) surfaces. Surface Science, 2016, 649, 72-79.	0.8	32
144	In situ scanning tunneling microscopy studies of the evolution of surface morphology and microstructure in epitaxial TiN(001) grown by ultra-high-vacuum reactive magnetron sputtering. Surface and Coatings Technology, 1997, 94-95, 403-408.	2.2	31

#	Article	IF	CITATIONS
145	Optimization ofin situsubstrate surface treatment in a cathodic arc plasma: A study by TEM and plasma diagnostics. Journal of Vacuum Science and Technology A: Vacuum, Surfaces and Films, 2001, 19, 1415-1420.	0.9	31
146	Growth and physical properties of epitaxial CeN layers on MgO(001). Journal of Applied Physics, 2003, 94, 921-927.	1.1	31
147	Electron/phonon coupling in group-IV transition-metal and rare-earth nitrides. Journal of Applied Physics, 2013, 114, .	1.1	31
148	Effects of incident N atom kinetic energy on TiN/TiN(001) film growth dynamics: A molecular dynamics investigation. Journal of Applied Physics, 2017, 121, .	1.1	31
149	Time evolution of ion fluxes incident at the substrate plane during reactive high-power impulse magnetron sputtering of groups IVb and VIb transition metals in Ar/N2. Journal of Vacuum Science and Technology A: Vacuum, Surfaces and Films, 2018, 36, .	0.9	31
150	Large-scale molecular dynamics simulations of TiN/TiN(001) epitaxial film growth. Journal of Vacuum Science and Technology A: Vacuum, Surfaces and Films, 2016, 34, .	0.9	30
151	Growth, nanostructure, and optical properties of epitaxial VN _x /MgO(001) (0.80 â‰ष्र â‰ष.00) layers deposited by reactive magnetron sputtering. Journal of Materials Chemistry C, 2016, 4, 7924-7938.	2.7	30
152	Reactive sputtering in the ABSTM system. Surface and Coatings Technology, 1993, 56, 179-182.	2.2	29
153	Epitaxial TiN(001) Grown and Analyzed In situ by XPS and UPS. I. Analysis of As-deposited Layers. Surface Science Spectra, 2000, 7, 193-203.	0.3	29
154	In-situ nanoindentation of epitaxial TiN/MgO (001) in a transmission electron microscope. Journal of Electronic Materials, 2003, 32, 1023-1027.	1.0	29
155	Ti and N adatom descent pathways to the terrace from atop two-dimensional TiN/TiN(001) islands. Thin Solid Films, 2014, 558, 37-46.	0.8	29
156	Combined steered arc-unbalanced magnetron grown niobium coatings for decorative and corrosion resistance applications. Surface and Coatings Technology, 1996, 82, 57-64.	2.2	28
157	Low-temperature growth of dense and hard Ti0.41Al0.51Ta0.08N films via hybrid HIPIMS/DC magnetron co-sputtering with synchronized metal-ion irradiation. Journal of Applied Physics, 2017, 121, .	1.1	28
158	Age hardening in superhard ZrB2-rich Zr1-xTaxBy thin films. Scripta Materialia, 2021, 191, 120-125.	2.6	28
159	Self-organized anisotropic (Zr1â~'Si)N nanocomposites grown by reactive sputter deposition. Acta Materialia, 2015, 82, 179-189.	3.8	27
160	Gas rarefaction effects during high power pulsed magnetron sputtering of groups IVb and VIb transition metals in Ar. Journal of Vacuum Science and Technology A: Vacuum, Surfaces and Films, 2017, 35, .	0.9	27
161	Recent developments in surface science and engineering, thin films, nanoscience, biomaterials, plasma science, and vacuum technology. Thin Solid Films, 2018, 660, 120-160.	0.8	27
162	Development of 111 texture in Al films grown on SiO2/Si(001) by ultrahighâ€vacuum primaryâ€ion deposition. Journal of Vacuum Science and Technology A: Vacuum, Surfaces and Films, 1996, 14, 346-351.	0.9	26

#	Article	IF	CITATIONS
163	Structure evolution and properties of TiAlCN/VCN coatings deposited by reactive HIPIMS. Surface and Coatings Technology, 2014, 257, 38-47.	2.2	26
164	Systematic compositional analysis of sputter-deposited boron-containing thin films. Journal of Vacuum Science and Technology A: Vacuum, Surfaces and Films, 2021, 39, .	0.9	26
165	Directed sputter deposition of AlCu: Film microstructure and microchemistry. Journal of Vacuum Science and Technology A: Vacuum, Surfaces and Films, 1994, 12, 3169-3175.	0.9	25
166	Morphology and microstructure of epitaxial Cu(001) films grown by primary ion deposition on Si and Ge substrates. Journal of Applied Physics, 1996, 80, 6699-6705.	1.1	25
167	TiAlCN/VCN nanolayer coatings suitable for machining of Al and Ti alloys deposited by combined high power impulse magnetron sputtering/unbalanced magnetron sputtering. Surface Engineering, 2010, 26, 610-614.	1.1	25
168	Si incorporation in Ti1â^'xSixN films grown on TiN(001) and (001)-faceted TiN(111) columns. Surface and Coatings Technology, 2014, 257, 121-128.	2.2	25
169	Enhanced Ti0.84Ta0.16N diffusion barriers, grown by a hybrid sputtering technique with no substrate heating, between Si(001) wafers and Cu overlayers. Scientific Reports, 2018, 8, 5360.	1.6	25
170	Single-phase polycrystalline Ti1â~'xWxN alloys (0⩽x⩽0.7) grown by UHV reactive magnetron sputtering: microstructure and physical properties. Thin Solid Films, 1994, 253, 445-450.	0.8	24
171	Control of the metal/gas ion ratio incident at the substrate plane during high-power impulse magnetron sputtering of transition metals in Ar. Thin Solid Films, 2017, 642, 36-40.	0.8	24
172	Improved oxidation properties from a reduced B content in sputter-deposited TiBx thin films. Surface and Coatings Technology, 2021, 420, 127353.	2.2	24
173	V0.5Mo0.5Nx/MgO(001): Composition, nanostructure, and mechanical properties as a function of film growth temperature. Acta Materialia, 2017, 126, 194-201.	3.8	23
174	Low temperature (<i>T</i> s/ <i>T</i> m < 0.1) epitaxial growth of HfN/MgO(001) via reactive HiPI with metal-ion synchronized substrate bias. Journal of Vacuum Science and Technology A: Vacuum, Surfaces and Films, 2018, 36, .	MS 0.9	23
175	Toward energy-efficient physical vapor deposition: Routes for replacing substrate heating during magnetron sputter deposition by employing metal ion irradiation. Surface and Coatings Technology, 2021, 415, 127120.	2.2	23
176	Decomposition of hexafluoroacetylacetonate Cu(I) vinyltrimethylsilane on, and diffusion of Cu into single crystal and polycrystalline titanium nitride. Surface Science, 1993, 295, 219-229.	0.8	22
177	IN-SITU HIGH-TEMPERATURE SCANNING-TUNNELING-MICROSCOPY STUDIES OF TWO-DIMENSIONAL ISLAND-DECAY KINETICS ON ATOMICALLY SMOOTH TiN(001). Surface Review and Letters, 2000, 07, 589-593.	0.5	22
178	Interfacial reactions in epitaxial Al/TiN(111) model diffusion barriers: Formation of an impervious self-limited wurtzite-structure AIN(0001) blocking layer. Journal of Applied Physics, 2001, 89, 7841-7845.	1.1	22
179	COmparison of Some Basic Plasma Parameters and Discharge Characteristics of Planar Magnetron Sputtering Discharges in Argon and Neon. Contributions To Plasma Physics, 1990, 30, 223-231.	0.5	21
180	Growth of TaC thin films by reactive direct current magnetron sputtering: Composition and structure. Journal of Vacuum Science and Technology A: Vacuum, Surfaces and Films, 1990, 8, 3769-3778.	0.9	21

#	Article	IF	CITATIONS
181	Epitaxial TiN(001) Grown and Analyzed In situ by XPS and UPS. II. Analysis of Ar+ Sputter Etched Layers. Surface Science Spectra, 2000, 7, 204-212.	0.3	21
182	In situ X-ray Photoelectron, Ultraviolet Photoelectron, and Auger Electron Spectroscopy Spectra from First-Row Transition-Metal Nitrides: ScN, TiN, VN, and CrN. Surface Science Spectra, 2000, 7, 167-168.	0.3	21
183	Nanophase films deposited from a high-rate, nanoparticle beam. Journal of Vacuum Science & Technology an Official Journal of the American Vacuum Society B, Microelectronics Processing and Phenomena, 2002, 20, 995.	1.6	21
184	Growth and physical properties of epitaxial metastable Hf1â^'xAlxN alloys deposited on MgO(001) by ultrahigh vacuum reactive magnetron sputtering. Surface and Coatings Technology, 2007, 202, 809-814.	2.2	21
185	Effect of off stoichiometry on Raman scattering from epitaxial and polycrystalline HfNx (0.85≤â‰\$.50) grown on MgO(001). Journal of Applied Physics, 2008, 104, 033507.	1.1	21
186	Low-temperature vapour–liquid–solid (VLS) growth of vertically aligned silicon oxide nanowires using concurrent ion bombardment. Nanotechnology, 2009, 20, 115607.	1.3	21
187	Microstructural characterization of thin SiOx films obtained by physical vapor deposition. Materials Science and Engineering B: Solid-State Materials for Advanced Technology, 2010, 174, 132-136.	1.7	21
188	Effects of surface vibrations on interlayer mass transport: <i>Ab initio</i> molecular dynamics investigation of Ti adatom descent pathways and rates from TiN/TiN(001) islands. Physical Review B, 2018, 97, .	1.1	21
189	High-power impulse magnetron sputter deposition of TiBx thin films: Effects of pressure and growth temperature. Vacuum, 2019, 169, 108884.	1.6	21
190	Where is the unpaired transition metal in substoichiometric diboride line compounds?. Acta Materialia, 2021, 204, 116510.	3.8	21
191	Multifunctional ZrB2-rich Zr1-xCrxBy thin films with enhanced mechanical, oxidation, and corrosion properties. Vacuum, 2021, 185, 109990.	1.6	21
192	Shortlisted substrate ion etching in combined steered cathodic arc–ubm deposition system: effects on interface architecture, adhesion, and tool performance. Surface Engineering, 2000, 16, 176-180.	1.1	20
193	Structural and mechanical properties of diamond-like carbon films deposited by direct current magnetron sputtering. Journal of Vacuum Science and Technology A: Vacuum, Surfaces and Films, 2003, 21, 851-859.	0.9	20
194	Combined filtered cathodic arc etching pretreatment–magnetron sputter deposition of highly adherent CrN films. Journal of Vacuum Science and Technology A: Vacuum, Surfaces and Films, 2007, 25, 543-550.	0.9	20
195	Real-time control of AlN incorporation in epitaxial Hf1â^'Al N using high-flux, low-energy (10–40 eV) ion bombardment during reactive magnetron sputter deposition from a Hf0.7Al0.3 alloy target. Acta Materialia, 2011, 59, 421-428.	3.8	20
196	X-ray Photoelectron Spectroscopy Analyses of the Electronic Structure of Polycrystalline Ti1-xAlxN Thin Films with 0 â‰ â €‰x â‰ â €‰0.96. Surface Science Spectra, 2014, 21, 35-49.	0.3	20
197	Interfacial reaction pathways and kinetics during annealing of epitaxial Al/TiN(001) model diffusion barrier systems. Thin Solid Films, 2001, 391, 69-80.	0.8	19
198	Phosphorus incorporation during Si(001):P gas-source molecular beam epitaxy: Effects on growth kinetics and surface morphology. Journal of Applied Physics, 2008, 103, 123530.	1.1	19

#	Article	IF	CITATIONS
199	Structural Properties of AlN Grown on Sapphire at Plasma Self-Heating Conditions Using Reactive Magnetron Sputter Deposition. Journal of Electronic Materials, 2010, 39, 1146-1151.	1.0	19
200	Nanodiamond-Based Nanolubricants. Fullerenes Nanotubes and Carbon Nanostructures, 2012, 20, 606-610.	1.0	19
201	Influence of the interface composition on the corrosion behavior of unbalanced magnetron grown niobium coatings on steel. Journal of Vacuum Science and Technology A: Vacuum, Surfaces and Films, 2001, 19, 1392-1398.	0.9	18
202	Structure and optical properties of (Al2O3)x(Tio)1â^'x thin films prepared by a sol–gel processing. Vacuum, 2004, 76, 215-218.	1.6	18
203	Synchrotron x-ray diffraction and transmission electron microscopy studies of interfacial reaction paths and kinetics during annealing of fully-002-textured Al/TiN bilayers. Journal of Vacuum Science and Technology A: Vacuum, Surfaces and Films, 2001, 19, 182-191.	0.9	17
204	Coalescence kinetics of two-dimensional TiN islands on atomically smooth TiN(001) and TiN(111) terraces. Surface Science, 2003, 540, L611-L616.	0.8	17
205	Self-organized lamellar structured tantalum–nitride by UHV unbalanced-magnetron sputtering. Thin Solid Films, 2005, 475, 45-48.	0.8	17
206	Raman scattering from epitaxial HfN layers grown on MgO(001). Journal of Applied Physics, 2006, 99, 043507.	1.1	17
207	Characterization studies of pulse magnetron sputtered hard ceramic titanium diboride coatings alloyed with silicon. Acta Materialia, 2008, 56, 4172-4182.	3.8	17
208	Oxidation kinetics of overstoichiometric TiB2 thin films grown by DC magnetron sputtering. Corrosion Science, 2022, 206, 110493.	3.0	17
209	Direct current reactive sputtering of aluminium. Thin Solid Films, 1978, 52, 365-371.	0.8	16
210	Atomic concentrations of binary compound thin films on elemental substrates determined by Rutherford backscattering techniques. Journal of Applied Physics, 1983, 54, 1358-1364.	1.1	16
211	Lowâ€energy (5 <ei<100 beam<br="" ev),="" for="" highâ€brightness,="" ion="" primary="" source="" ultrahigh="" vacuum="">deposition: Applications for Al and Ge. Journal of Vacuum Science and Technology A: Vacuum, Surfaces and Films, 1995, 13, 2836-2842.</ei<100>	0.9	16
212	Al/TixW1â^'x metal/diffusion-barrier bilayers: Interfacial reaction pathways and kinetics during annealing. Journal of Applied Physics, 1997, 82, 2312-2322.	1.1	16
213	Evolution of nanoscale texture in ultrathin TiN films. Applied Physics Letters, 2001, 78, 2223-2225.	1.5	16
214	Sublimation of Atomic Layers from a Chromium Surface. Physical Review Letters, 2006, 96, 126106.	2.9	16
215	Fully strained low-temperature epitaxy of TiN/MgO(001) layers using high-flux, low-energy ion irradiation during reactive magnetron sputter deposition. Thin Solid Films, 2010, 518, 5169-5172.	0.8	16
216	Imaging suspended carbon nanotubes in field-effect transistors configured with microfabricated slits for transmission electron microscopy. Applied Physics Letters, 2005, 87, 173108.	1.5	15

#	Article	IF	CITATIONS
217	Epitaxial V0.6W0.4N/MgO(001): Evidence for ordering on the cation sublattice. Journal of Vacuum Science and Technology A: Vacuum, Surfaces and Films, 2013, 31, .	0.9	15
218	Growth and mechanical properties of 111-oriented V0.5Mo0.5Nx/Al2O3(0001) thin films. Journal of Vacuum Science and Technology A: Vacuum, Surfaces and Films, 2018, 36, .	0.9	15
219	Self-organized columnar Zr0.7Ta0.3B1.5 core/shell-nanostructure thin films. Surface and Coatings Technology, 2020, 401, 126237.	2.2	15
220	Towards energy-efficient physical vapor deposition: Mapping out the effects of W+ energy and concentration on the densification of TiAlWN thin films grown with no external heating. Surface and Coatings Technology, 2021, 424, 127639.	2.2	15
221	Raman spectroscopy study of C/Cr coatings deposited by the combined steered cathodic ARC/unbalanced magnetron sputtering technique. Surface and Coatings Technology, 2005, 200, 1117-1122.	2.2	14
222	Growth of CoSi2 on Si(001) by reactive deposition epitaxy. Journal of Applied Physics, 2005, 97, 044909.	1.1	14
223	The influence of pressure and magnetic field on the deposition of epitaxial TiBx thin films from DC magnetron sputtering. Vacuum, 2020, 177, 109355.	1.6	14
224	Effect of ion bombardment during growth on the electrical resistivity of magnetron-sputtered carbon films. Thin Solid Films, 1989, 168, 239-248.	0.8	13
225	Morphology and microstructure of tensile-strained SiGe(001) thin epitaxial films. Journal of Applied Physics, 1998, 83, 1096-1102.	1.1	13
226	Quantitative C lattice site distributions in epitaxial Ge1â^'yCy/Ge(001) layers. Journal of Applied Physics, 2001, 90, 3910-3918.	1.1	13
227	Growth of dense, hard yet low-stress Ti0.40Al0.27W0.33N nanocomposite films with rotating substrate and no external substrate heating. Journal of Vacuum Science and Technology A: Vacuum, Surfaces and Films, 2020, 38, .	0.9	13
228	Deposition of carbon films by bias magnetron sputtering in neon and argon. Thin Solid Films, 1990, 185, 247-256.	0.8	12
229	Interfacial reaction pathways and kinetics during annealing of 111-textured Al/TiN bilayers: A synchrotron x-ray diffraction and transmission electron microscopy study. Journal of Vacuum Science and Technology A: Vacuum, Surfaces and Films, 2001, 19, 2207-2216.	0.9	12
230	Sputter-cleaned Epitaxial VxMo(1-x)Ny/MgO(001) Thin Films Analyzed by X-ray Photoelectron Spectroscopy: 1. Single-crystal V0.48Mo0.52N0.64. Surface Science Spectra, 2013, 20, 68-73.	0.3	12
231	The dynamics of TiNx (x = 1–3) admolecule interlayer and intralayer transport on TiN/TiN(001) islands. Thin Solid Films, 2015, 589, 133-144.	0.8	12
232	Synthesis and characterization of CrB2 thin films grown by DC magnetron sputtering. Scripta Materialia, 2021, 200, 113915.	2.6	12
233	Ion energy distributions in reactive arc evaporation discharges used for deposition of TiN films. Surface and Coatings Technology, 1997, 92, 150-156.	2.2	11
234	Ion-induced surface relaxation: controlled bending and alignment of nanowire arrays. Nanotechnology, 2012, 23, 175302.	1.3	11

#	Article	IF	CITATIONS
235	Sputter-cleaned Epitaxial VxMo(1-x)Ny/MgO(001) Thin Films Analyzed by X-ray Photoelectron Spectroscopy: 2. Single-crystal V0.47Mo0.53N0.92. Surface Science Spectra, 2013, 20, 74-79.	0.3	11
236	Thermally induced structural evolution and age-hardening of polycrystalline V1–xMoxN (xÂâ‰^Â0.4) thin films. Surface and Coatings Technology, 2021, 405, 126723.	2.2	11
237	Epitaxial CrN(001) Grown and Analyzed In situ by XPS and UPS. I. Analysis of As-deposited Layers. Surface Science Spectra, 2000, 7, 250-261.	0.3	10
238	Directed nanostructural evolution in Ti0.8Ce0.2N layers grown as a function of low-energy, high-flux ion irradiation. Applied Physics Letters, 2004, 84, 2796-2798.	1.5	10
239	Directed Self-Assembly of Ge Nanostructures on Very High Index, Highly Anisotropic Si(hkl) Surfaces. Nano Letters, 2005, 5, 369-372.	4.5	10
240	Hierarchically textured Li Mn2â^'O4 thin films as positive electrodes for lithium-ion batteries. Journal of Power Sources, 2012, 206, 288-294.	4.0	10
241	Cubic-structure Al-rich TiAlSiN thin films grown by hybrid high-power impulse magnetron co-sputtering with synchronized Al+ irradiation. Surface and Coatings Technology, 2020, 385, 125364.	2.2	10
242	A Microelectromechanical System for Nano-Scale Testing of One Dimensional Nanostructures. Sensor Letters, 2008, 6, 76-87.	0.4	10
243	Influence of the Basic Process Parameters on the Ion/Atom Arrival Rate Ratio during Magnetron Sputter Deposition of Thin Carbon Films. Contributions To Plasma Physics, 1988, 28, 265-273.	0.5	9
244	Epitaxial VN(001) Grown and Analyzed In situ by XPS and UPS. I. Analysis of As-deposited Layers. Surface Science Spectra, 2000, 7, 221-232.	0.3	9
245	Epitaxial ScN(001) Grown and Analyzed In situ by XPS and UPS. II. Analysis of Ar+ Sputter Etched Layers. Surface Science Spectra, 2000, 7, 178-184.	0.3	9
246	Role of fast sputtered particles during sputter deposition: Growth of epitaxialGe0.99C0.01/Ge(001). Physical Review B, 2000, 62, 11203-11208.	1.1	9
247	Optical properties of nanophase films measured by variable-angle spectroscopic ellipsometry. Thin Solid Films, 2002, 408, 211-217.	0.8	9
248	Nanoparticle beam formation and investigation of gold nanostructured films. Journal of Vacuum Science & Technology an Official Journal of the American Vacuum Society B, Microelectronics Processing and Phenomena, 2003, 21, 2313.	1.6	9
249	Epitaxial growth of CoSi2 on Si(001) by reactive deposition epitaxy: Island growth and coalescence. Thin Solid Films, 2006, 515, 1340-1348.	0.8	9
250	Self-structuring in Zr1â^'xAlxN films as a function of composition and growth temperature. Scientific Reports, 2018, 8, 16327.	1.6	9
251	Dense Ti0.67Hf0.33B1.7 thin films grown by hybrid HfB2-HiPIMS/TiB2-DCMS co-sputtering without external heating. Vacuum, 2021, 186, 110057.	1.6	9
252	Experimental Methods and Data Analysis for Fluctuation Microscopy. Materials Research Society Symposia Proceedings, 1999, 589, 155.	0.1	8

#	Article	IF	CITATIONS
253	Epitaxial metastable Ge1â^'yCy (y⩽0.02) alloys grown on Ge(001) from hyperthermal beams: C incorporation and lattice sites. Journal of Applied Physics, 2000, 88, 96-104.	1.1	8
254	YBCO/LSMO and LSMO/YBCO double-layer deposition by off-axis magnetron sputtering and strain effects. Vacuum, 2002, 69, 243-247.	1.6	8
255	Experimental evidence for a dissociation mechanism in NH3 detection with MIS field-effect devices. Sensors and Actuators B: Chemical, 2003, 89, 1-8.	4.0	8
256	Sputter-cleaned Epitaxial VxMo(1-x)Ny/MgO(001) Thin Films Analyzed by X-ray Photoelectron Spectroscopy: 3. Polycrystalline V0.49Mo0.51N1.02. Surface Science Spectra, 2013, 20, 80-85.	0.3	8
257	Dense, single-phase, hard, and stress-free Ti0.32Al0.63W0.05N films grown by magnetron sputtering with dramatically reduced energy consumption. Scientific Reports, 2022, 12, 2166.	1.6	8
258	Angular distribution and sputtering yield of Al and Al2O3 during 40 key argon ion bombardment. Vacuum, 1982, 32, 747-752.	1.6	7
259	Growth and microstructure of epitaxial 45°-rotated bcc W layers on NaCl-structure MgO(001) substrates and TiN(001) buffer layers. Journal of Crystal Growth, 1992, 123, 344-356.	0.7	7
260	Continuum model of thin film deposition incorporating finite atomic length scales. Journal of Applied Physics, 2002, 92, 3487-3494.	1.1	7
261	Electromigration in epitaxial Cu(001) lines. AlP Conference Proceedings, 2002, , .	0.3	7
262	Determination of absolute orientation-dependent TiN(001) and TiN(111) step energies. Vacuum, 2004, 74, 345-351.	1.6	7
263	Orientation-dependent mobilities from analyses of two-dimensional TiN(111) island decay kinetics. Thin Solid Films, 2006, 510, 339-345.	0.8	7
264	Influence of ion bombardment on structure and tribological performance of nanoscale multilayer C/Cr PVD coatings. Surface Engineering, 2006, 22, 92-98.	1.1	7
265	Real-time imaging of surface evolution driven by variable-energy ion irradiation. Ultramicroscopy, 2008, 108, 646-655.	0.8	7
266	LEEM investigations of surfaces using a beam of energetic selfâ€ions. Microscopy Research and Technique, 2009, 72, 197-207.	1.2	7
267	Formation of Si Nanocrystals in Thin SiO ₂ Films for Memory Device Applications. Materials Science Forum, 2010, 644, 101-104.	0.3	7
268	Novel hard, tough HfAlSiN multilayers, defined by alternating Si bond structure, deposited using modulated high-flux, low-energy ion irradiation of the growing film. Journal of Vacuum Science and Technology A: Vacuum, Surfaces and Films, 2015, 33, .	0.9	7
269	TiN film growth on misoriented TiN grains with simultaneous low-energy bombardment: Restructuring leading to epitaxy. Thin Solid Films, 2019, 688, 137380.	0.8	7

270 X-ray photoelectron spectroscopy analysis of TiBx (1.3 â‰â€‰x â‰â€‰3.0) thin films. Journal of Vacuum Science and Technology A: Vacuum, Surfaces and Films, 2021, 39, .

#	Article	IF	CITATIONS
271	Oxidation resistance and mechanical properties of sputter-deposited Ti0.9Al0.1B2-y thin films. Surface and Coatings Technology, 2022, 442, 128187.	2.2	7
272	Reaction paths and kinetics of aluminide formation in Al/epitaxialâ€W(001) model diffusion barrier systems. Journal of Applied Physics, 1995, 78, 194-203.	1.1	6
273	A Comparison of Auger Electron Spectra from Stoichiometric Epitaxial TiN(001) After (1) UHV Cleaving and (2) Ar+ Sputter Etching. Surface Science Spectra, 2000, 7, 93-100.	0.3	6
274	Magnetic and electric properties of magnetron-sputtered YBCO/LSMO and LSMO/YBCO double layers. Vacuum, 2004, 76, 261-264.	1.6	6
275	Expansion and melting of Xe nanocrystals in Si. Physical Review B, 2006, 74, .	1.1	6
276	Effect of oxygen to argon ratio on the properties of thin SiO x films deposited by r.f. sputtering. Journal of Materials Science: Materials in Electronics, 2010, 21, 481-485.	1.1	6
277	Importance of line and interfacial energies during VLS growth of finely stranded silica nanowires. Journal of Materials Research, 2011, 26, 2247-2253.	1.2	6
278	Formation of Defects During Ion-Assisted Growth of Thin Films from the Vapor Phase. Materials Research Society Symposia Proceedings, 1992, 268, 71.	0.1	5
279	Epitaxial CrN(001) Grown and Analyzed In situ by XPS and UPS. II. Analysis of Ar+ Sputter Etched Layers. Surface Science Spectra, 2000, 7, 262-270.	0.3	5
280	Epitaxial VN(001) Grown and Analyzed In situ by XPS and UPS. II. Analysis of Ar+ Sputter Etched Layers. Surface Science Spectra, 2000, 7, 233-241.	0.3	5
281	Nucleation and growth kinetics of spiral steps on TiN(111): Anin situlow-energy electron microscopy study. Journal of Applied Physics, 2005, 98, 034901.	1.1	5
282	Elastic buckling of AlN ribbons on elastomeric substrate. Applied Physics Letters, 2009, 94, 092104.	1.5	5
283	The Si3N4/TiN Interface: 1. TiN(001) Grown and Analyzed <i>In situ</i> using Angle-resolved X-ray Photoelectron Spectroscopy. Surface Science Spectra, 2012, 19, 33-41.	0.3	5
284	Reflection thermal diffuse x-ray scattering for quantitative determination of phonon dispersion relations. Physical Review B, 2015, 92, .	1.1	5
285	Corrosion Resistant TiTaN and TiTaAlN Thin Films Grown by Hybrid HiPIMS/DCMS Using Synchronized Pulsed Substrate Bias with No External Substrate Heating. Coatings, 2019, 9, 841.	1.2	5
286	Electromigration in Epitaxial Copper Lines. Materials Research Society Symposia Proceedings, 2000, 648, 1.	0.1	4
287	Epitaxial ScN(001) Grown and Analyzed In situ by XPS and UPS. I. Analysis of As-deposited Layers. Surface Science Spectra, 2000, 7, 169-177.	0.3	4
288	CoSi2 growth on Si(001) by reactive deposition epitaxy: Effects of high-flux, low-energy ion irradiation. Journal of Applied Physics, 2006, 100, 013510.	1.1	4

#	Article	IF	CITATIONS
289	TiN surface dynamics: role of surface and bulk mass transport processes. AIP Conference Proceedings, 2007, , .	0.3	4
290	Improving oxidation and wear resistance of TiB2 films by nano-multilayering with Cr. Surface and Coatings Technology, 2022, 436, 128337.	2.2	4
291	On the nature of planar defects in transition metal diboride line compounds. Materialia, 2022, 24, 101478.	1.3	4
292	Aluminide formation in polycrystalline Al/W metal/barrier thin-film bilayers: Reaction paths and kinetics. Journal of Applied Physics, 1997, 82, 201-209.	1.1	3
293	Ion-Implanted Amorphous Silicon Studied by Variable Coherence TEM. Materials Research Society Symposia Proceedings, 1999, 589, 247.	0.1	3
294	Channeling-induced asymmetric distortion of depth profiles from polycrystalline-TiN/Ti/TiN(001) trilayers during secondary ion mass spectrometry. Journal of Vacuum Science & Technology an Official Journal of the American Vacuum Society B, Microelectronics Processing and Phenomena, 2000, 18, 1369.	1.6	3
295	Self-hardening of Nanocrystalline Ti-B-N Thin Films. Microscopy and Microanalysis, 2006, 12, 720-721.	0.2	3
296	The Si3N4/TiN Interface: An Introduction to a Series of Ultrathin Films Grown and Analyzed <i>In situ</i> using X-ray Photoelectron Spectroscopy. Surface Science Spectra, 2012, 19, 30-32.	0.3	3
297	In situ high-temperature scanning tunneling microscopy study of bilayer graphene growth on 6H-SiC(0001). Thin Solid Films, 2012, 520, 5289-5293.	0.8	3
298	Effect of low-energy ion assistance on the properties of sputtered ZrB2 films. Vacuum, 2022, 195, 110688.	1.6	3
299	Microstructure, mechanical, and corrosion properties of Zr1-xCrxBy diboride alloy thin films grown by hybrid high power impulse/DC magnetron co-sputtering. Applied Surface Science, 2022, 591, 153164.	3.1	3
300	Epitaxial TiN(001) Grown and Analyzed In situ by AES After (1) Deposition and (2) Ar+ Sputter Etching. Surface Science Spectra, 2000, 7, 213-220.	0.3	2
301	Texture of Al thin films deposited by magnetron sputtering onto epitaxial W(001). Journal of Applied Physics, 2000, 87, 168-171.	1.1	2
302	Deposition and Properties of Thin (ZrO2)x(Al2O3)1-x Films on Silicon. Plasma Processes and Polymers, 2006, 3, 179-183.	1.6	2
303	Enhanced Ge/Si(001) island areal density and self-organization due to P predeposition. Journal of Applied Physics, 2011, 109, 093526.	1.1	2
304	The Si3N4/TiN Interface: 3. Si3N4/TiN(001) Grown with a â^'150 V Substrate Bias and Analyzed <i>In situ</i> using Angle-resolved X-ray Photoelectron Spectroscopy. Surface Science Spectra, 2012, 19, 52-61.	0.3	2
305	Role of ethylene on surface oxidation of TiO2(110). Applied Physics Letters, 2012, 101, 211601.	1.5	2
306	Reprint of: Improving oxidation and wear resistance of TiB2 films by nano-multilayering with Cr. Surface and Coatings Technology, 2022, 442, 128602.	2.2	2

#	Article	IF	CITATIONS
307	Quantitative compositional depth profiling of Si1â^'xâ^'yGexCy thin films by simultaneous elastic recoil detection and Rutherford backscattering spectrometry. Nuclear Instruments & Methods in Physics Research B, 1998, 136-138, 654-660.	0.6	1
308	Analysis of the Atomic Scale Defect Chemistry in Oxygen Deficient Materials by STEM. Materials Research Society Symposia Proceedings, 1999, 589, 69.	0.1	1
309	Epitaxial ScN(001) Grown and Analyzed In situ by AES After (1) Deposition and (2) Ar+ Sputter Etching. Surface Science Spectra, 2000, 7, 185-192.	0.3	1
310	Epitaxial VN(001) Grown and Analyzed In situ by AES After (1) Deposition and (2) Ar+ Sputter Etching. Surface Science Spectra, 2000, 7, 242-249.	0.3	1
311	Microstructure, Oxidation and Tribological Properties of TiAlCN/VCN Coatings Deposited by Reactive HIPIMS. IOP Conference Series: Materials Science and Engineering, 2012, 39, 012011.	0.3	1
312	The Si3N4/TiN Interface: 7. Ti/TiN(001) Grown and Analyzed <i>In situ</i> using X-ray Photoelectron Spectroscopy. Surface Science Spectra, 2012, 19, 92-97.	0.3	1
313	The Si3N4/TiN Interface: 2. Si3N4/TiN(001) Grown with a â^'7 V Substrate Bias and Analyzed In situ using Angle-resolved X-ray Photoelectron Spectroscopy. Surface Science Spectra, 2012, 19, 42-51.	0.3	1
314	The Si3N4/TiN Interface: 4. Si3N4/TiN(001) Grown with a â^'250 V Substrate Bias and Analyzed <i>In situ</i> using Angle-resolved X-ray Photoelectron Spectroscopy. Surface Science Spectra, 2012, 19, 62-71.	0.3	1
315	Mechanical properties of VMoNO as a function of oxygen concentration: Toward development of hard and tough refractory oxynitrides. Journal of Vacuum Science and Technology A: Vacuum, Surfaces and Films, 2019, 37, .	0.9	1
316	The mechanism of d.c. reactive sputtering. Thin Solid Films, 1981, 85, 300.	0.8	0
317	The dc magnetron sputter deposition process of YBa 2 Cu 3 O x thin films. Physica C: Superconductivity and Its Applications, 1989, 162-164, 599-600.	0.6	0
318	Influence of the Plasma Kinetics on the Si/C Ratio of a‣i _{<i>x</i>} C _{1â€<i>x</i>} : H Thin Films Deposited by Reactive Magnetron Sputtering of a Si Target in Ar + CH ₄ Gas Mixtures. Contributions To Plasma Physics, 1994, 34, 39-49.	0.5	0
319	Epitaxial CrN(001) Grown and Analyzed In situ by AES After (1) Deposition and (2) Ar+ Sputter Etching. Surface Science Spectra, 2000, 7, 271-278.	0.3	0
320	Progress towards Quantitative Electron Nanodiffraction. Microscopy and Microanalysis, 2002, 8, 658-659.	0.2	0
321	Quantitative structure determination of individual carbon nanotubes using nano-area electron diffraction. Microscopy and Microanalysis, 2003, 9, 322-323.	0.2	0
322	Electrical characterization of MOS structures with self-organized three-layer gate dielectric containing Si nanocrystals. Journal of Physics: Conference Series, 2010, 253, 012034.	0.3	0
323	ICMCTF 2010. Surface and Coatings Technology, 2010, 205, 1177.	2.2	0
324	ICMCTF 2011 — Preface. Surface and Coatings Technology, 2011, 206, 1511.	2.2	0

#	Article	IF	CITATIONS
325	The Si3N4/TiN Interface: 5. TiN/Si3N4 Grown and Analyzed <i>In situ</i> using Angle-resolved X-ray Photoelectron Spectroscopy. Surface Science Spectra, 2012, 19, 72-81.	0.3	0
326	The Si3N4/TiN Interface: 6. Si/TiN(001) Grown and Analyzed <i>In situ</i> using Angle-resolved X-ray Photoelectron Spectroscopy. Surface Science Spectra, 2012, 19, 82-91.	0.3	0
327	ICMCTF 2013 — Preface. Thin Solid Films, 2013, 549, 1.	0.8	0
328	Preface of the special issue "Thin Films Advances―dedicated to the 75th birthday of Professor Joe Greene. Thin Solid Films, 2019, 688, 137494.	0.8	0
329	Feature-Scale to Wafer-Scale Modeling and Simulation of Physical Vapor Deposition. The IMA Volumes in Mathematics and Its Applications, 2004, , 219-236.	0.5	0
330	Preface for the Festschrift Honoring Dr. Steve Rossnagel. Journal of Vacuum Science and Technology A: Vacuum, Surfaces and Films, 2020, 38, .	0.9	0
331	Study of High Surface Area Alumina and Ga-Alumina Materials for Denox Catalyst Applications. Ceramic Engineering and Science Proceedings, 0, , 499-504.	0.1	0